Histol Histopathol (2023) 38: 1129-1143

Histology and Histopathology
From Cell Biology to Tissue Engineering

ORIGINAL ARTICLE Open Access

Circ_0000284 facilitates the growth, metastasis and glycolysis of intrahepatic cholangiocarcinoma through miR-152-3p-mediated PDK1 expression

Jian Sun[1]*, Menglong Feng[1]*, Huilian Zou[2], Yanping Mao[1] and Wei Yu[1]

[1]Department II of General Surgery and [2]Department of Gynaecology and Obstetrics, Hanchuan People's Hospital, Hanchuan, Hubei, China

*These authors contributed equally to this paper

Summary. Background. Circular RNAs (circRNAs) are key molecules in the regulation of intrahepatic cholangiocarcinoma (ICC) progression. The purpose of this study was to analyze the function and underlying molecular mechanism of circ_0000284 in ICC.

Methods. Quantitative real-time PCR was used to analyze the circ_0000284, microRNA (miR)-152-3p and pyruvate dehydrogenase kinase 1 (PDK1) expression. Cell proliferation, apoptosis, invasion and migration were executed by cell counting kit 8 assay, EdU assay, flow cytometry, transwell assay and wound healing assay, respectively. All protein expression levels were examined using western blot analysis. Cell glycolysis was analyzed by detecting glucose consumption, lactate production and ATP/ADP ratios. Target relationship was estimated by dual-luciferase reporter assay. The effect of circ_0000284 on ICC tumor growth *in vivo* was evaluated by constructing xenograft mice model.

Results. We detected high expression of circ_0000284 in ICC tumor tissues and cells. Downregulated circ_0000284 inhibited ICC cell proliferation, invasion, migration, glycolysis, and accelerated apoptosis. MiR-152-3p was sponged by circ_0000284, and its inhibitor revoked the effect of circ_0000284 knockdown on ICC cell progression. PDK1 was a target of miR-152-3p, and its expression was suppressed by circ_0000284 knockdown. PDK1 overexpression reversed the inhibition effect of miR-152-3p on ICC cell growth, metastasis and glycolysis. In animal experiments, circ_0000284 downregulation also inhibited ICC tumor growth.

Conclusion. Circ_0000284 promoted the growth, metastasis and glycolysis of ICC by miR-152-3p/PDK1 pathway, showing that circ_0000284 was a potential therapeutic target for ICC.

Key words: Intrahepatic cholangiocarcinoma, circ_0000284, miR-152-3p, PDK1

Corresponding Author: Wei Yu, Department II of General Surgery, Hanchuan People's Hospital, No.1, Renmin Avenue, Hanchuan, Hubei, 431600, China. e-mail: yuwei19811110@163.com

www.hh.um.es. DOI: 10.14670/HH-18-544

Introduction

Intrahepatic cholangiocarcinoma (ICC) refers to a malignant tumor originating from the secondary bile duct and its branch epithelium, which is a type of primary liver cancer (Zhang et al., 2016; El-Diawany et al., 2019). It is currently believed that surgery is the preferred treatment for prolonging the survival period of ICC. Unfortunately, due to the high recurrence rate, the clinical treatment results of ICC patients are still not satisfactory (Mavros et al., 2014; Lee and Chun, 2018). Molecular targeted therapy can kill tumor cells by inhibiting specific molecules that promote tumor development, and has become a research hotspot in ICC therapy (Hogdall et al., 2016; Moeini et al., 2016). It is necessary to clarify the pathological mechanism of ICC to explore new molecular targeted therapy strategies.

Circular RNAs (circRNAs) are endogenous non-coding RNAs, and their sequences are highly conserved and highly stable *in vivo* (Chen and Huang, 2018; Chen, 2020). CircRNA can competitively bind microRNA (miRNA), thereby reducing the inhibition of miRNA on its target, which is also called a ceRNA mechanism (Wu et al., 2019; Liu et al., 2020). In terms of function, circRNA plays a vital role in cardiovascular diseases, neurological diseases, and cancer (Li et al., 2017; Altesha et al., 2019). Research in recent years has provided a lot of evidence for circRNA as a potential molecular target for cancer diagnosis, prognosis and treatment (Lei et al., 2019; Li et al., 2020a,b). In ICC, circACTN4 had been found to enhance cell proliferation and metastasis to promote cancer progression by the miR-424-5p/YBX1 pathway, suggesting that circACTN4

might be a target for ICC treatment (Chen et al., 2021). Also, studies had reported that circHMGCS1-016 had increased expression in ICC tissues, which was correlated with patients' poor survival and could accelerate ICC cell proliferation and invasion via miR-1236-3p/CD73/GAL-8 (Xu et al., 2021).

Circ_0000284 is located at chr11: 33307958-33309057 and is originated from the HIPK3 gene. Previous studies had shown that circ_0000284 functioned with an oncogenic role in many cancers, and its high expression promoted the malignant phenotype of cancers, such as breast cancer (Qi et al., 2021) and lung cancer (Li et al., 2020b). It was reported that circ_0000284 was overexpressed in cholangiocarcinoma tissues, and it was able to facilitate cancer cell proliferation and metastasis (Wang et al., 2019). Therefore, we believed that circ_0000284 might be a key regulator for cholangiocarcinoma progression. Of course, the role of circ_0000284 in ICC progression needs to be further elucidated, and its potential molecular mechanism remains to be revealed. Based on these problems, we conducted this study, hoping to provide a reliable molecular target for ICC treatment.

Materials and methods

Samples

From March 2012 to April 2015, 29 ICC patients were recruited in Hanchuan People's Hospital through online and on-site methods. Inclusion criteria: pathological diagnosis was ICC. Exclusion criteria: no surgical resection; incomplete clinical data or follow-up data; accompanied by other diseases or malignant tumors. In total, 29 paired ICC tumor tissues and adjacent normal tissues were collected from ICC patients at Hanchuan People's Hospital. The tissue samples were stored directly at -80°C for the detection of target gene and protein. Some fresh tissue was used to prepare paraffin sections for H&E staining. For this study, all patients signed written informed consent and agreed to a 5-year follow-up. The clinicopathologic parameters of ICC patients are listed in Table 1. Our study was conducted at Hanchuan People's Hospital and was approved by the Ethics committee of the Hanchuan People's Hospital.

Immunohistochemical (IHC) staining

Paraffin-embedded fresh ICC tumor tissues and adjacent normal tissues were cut into slices 4 μm thick. After antigen recovery in a citrate buffer, the sections were incubated with primary antibody against Ki67 (ab15580, 1:100, Abcam, Cambridge, CA, USA) or PDK1 (1:100, ab227682, Abcam) at 4°C overnight and then incubated with HRP conjugated Goat anti-Rabbit IgG (1:50,000, ab205718, Abcam). DAB reagents (Beyotime, Shanghai, China) and hematoxylin (Solarbio, Beijing, China) were then used to stain the tissues. The staining results were recorded under a microscope.

Cell culture and transfection

ICC cell lines (RBE and HCCC-9810) and normal intrahepatic biliary epithelial cells (HIBEC) were bought from Procell (Wuhan, china), and the other two ICC cell lines (QBC-939 and HUCCT1) were obtained from JCRB (Osaka, Japan). All cells were cultured at 37°C with 5% CO_2 in RPMI-1640 medium (Gibco, Grand Island, NY, USA) added with 10% FBS (Gibco) and 1% streptomycin-penicillin (Gibco). The circ_0000284 small interference RNA (si-circ_0000284), pCD5 overexpression vector or lentivirus short hairpin RNA (sh-circ_0000284), miR-152-3p mimic or inhibitor (anti-miR-152-3p), pcDNA pyruvate dehydrogenase kinase 1 (PDK1) overexpression vector, and their controls were synthesized from GenePharma (Guangzhou, China). They were transfected into ICC cells with Lipofectamine 3000 reagent (Invitrogen, Carlsbad, CA, USA).

Quantitative real-time PCR (qRT-PCR)

Total RNA was extracted by RNeasy Mini Kit (Qiagen, Hilden, Germany) and then treated with or without RNase R solution for 15 min to assess the resistance of circ_0000284 on RNase R digestion. RNA was reverse-transcribed to cDNA by QuantiTect RT Kit (Qiagen). SYBR Green Master Mix (Vazyme, Nanjing, China) was used to determine target gene expression with specific primers. Primer sequences are exhibited in Table 2. Data were normalized to β-actin or U6 by the $2^{-\Delta\Delta Ct}$ method. Additionally, PARIS Kit (Invitrogen) was used to isolate cytoplasm RNA and nuclear RNA, and then circ_0000284 expression in cytoplasm and nucleus was detected.

Table 1. Correlation between the clinicopathologic parameters of ICC patients and circ_0000284 expression.

Parameter	Case	Circ_0000284 expression		P value
		Low (n=14)	High (n=15)	
Age (years)				0.55
≤60	12	5	7	
>60	17	9	8	
Gender				0.198
Female	13	8	5	
Male	16	6	10	
LNM				0.014*
NO	16	11	5	
Yes	13	3	10	
TNM stages				0.316
I-II	18	10	8	
III	11	4	7	

LNM, lymph node metastasis; TNM, tumor node metastasis; *P<0.05.

Cell counting kit 8 (CCK8) assay

ICC cells were seeded into 96-well plates and cultured for 48h. Afterwards, cells were incubated with CCK8 reagent (Sangon, Shanghai, China) for 4h. Cell viability was assessed via testing absorbance at 450 nm using microplate reader.

EdU assay

In line with the instructions of EdU cell proliferation Kit (Sangon), ICC cells were stained with EdU solution and DAPI solution. Cell images were captured under a fluorescence microscope to calculate EdU positive cell rate.

Flow cytometry

After transfection for 48h, ICC cells were harvested and suspended with binding buffer. Cell suspensions were treated with fluorescently labelled Annexin V-FITC reagent and PI reagent. Cell apoptosis rate was analyzed using flow cytometer.

Transwell assay

ICC cells suspended with serum-free medium were seeded into the upper of Matrigel-coated transwell chambers (Costar, Cambridge, MA, USA). Serum medium was added into the bottom chamber. 24h later, cells that invaded into bottom surface were immobilized and stained. Five fields were randomly selected to calculate invasive cell numbers.

Wound healing assay

ICC cells in 6-well plates were cultured until 90% confluence. Cells were scratched with a sterile pipette tip and cultured with serum-free medium for 24h. The wound area was measured to calculate migration distance.

Determination of cell glycolysis

Glucose consumption, lactate production and ATP/ADP ratios were determined by Commercial Kits (Abcam) based on the manufacturers' protocols.

Western blot (WB) analysis

After obtaining protein using RIPA lysis buffer (Beyotime), the same amount of protein was loaded into SDS-PAGE gel and transferred onto PVDF membranes. Non-fat milk was used to block the membrane, and then the membrane was hatched with primary and secondary antibodies. Protein signals were detected using ECL Chemiluminescence Kit (Beyotime). All antibodies were bought from Abcam and shown as below: anti-cleaved-caspase-3 (1:1,000, ab2302), anti-MMP9 (1:1,000, ab38898), anti-PDK1 (1:2,000, ab207450), anti-β-actin (1:1,000, ab8227), and Goat anti-Rabbit IgG (1:50,000, ab205718).

Dual-luciferase reporter assay

The wild-type/mutant-type circ_0000284 (WT/MUT-circ_0000284) or PDK1 3'UTR (WT/MUT-PDK1 3'UTR) vectors were constructed by cloning their sequences into pGL3 luciferase reporter vectors. Then, the generated vectors were transfected into ICC cells with miR-152-3p mimic/miR-NC. Luciferase activities were analyzed using Dual-Luciferase Reporter Gene Assay Kit (Beyotime).

Mouse xenograft models

The animal study was approved by the Animal Ethics committee of the Hanchuan People's Hospital and was carried out in accordance with the animal experimentation guidelines in China. HUCCT1 cells were transfected with sh-circ_0000284/sh-NC for 48 h, and then subcutaneously injected into BALB/c nude mice (n=6 per group; Vital River, Beijing, China). Tumor volume was measured every 3 days after injection for 7 days. 22 days later, the mice were euthanized and the tumor tissues were collected for photographing and weighting. Subsequently, the tumor tissue was used to detect target gene and protein expression, and prepare paraffin sections for IHC staining.

Table 2. Primer sequences used for qRT-PCR.

Name		Primers (5'-3')
Circ_0000284	Forward	GGCAGCCTTACAGGGTTAAA
	Reverse	GGGTAGACCAAGACTTGTGAGG
HIPK3	Forward	TCACAAGTCTTGGTCTACCCA
	Reverse	CACATAGGTCCGTGGATAGTTTC
miR-152-3p	Forward	GCCGAGTCAGTGCATGACAGA
	Reverse	ATCCAGTGCAGGGTCCGAGG
PDK1	Forward	CTGTGATACGGATCAGAAACCG
	Reverse	TCCACCAAACAATAAAGAGTGCT
GAPDH	Forward	CTCTGCTCCTCCTGTTCGAC
	Reverse	CGACCAAATCCGTTGACTCC
β-actin	Forward	CTCCATCCTGGCCTCGCTGT
	Reverse	GCTGTCACCTTCACCGTTCC
U6	Forward	CTCGCTTCGGCAGCACA
	Reverse	AACGCTTCACGAATTTGCGT
P21	Forward	TGCCGAAGTCAGTTCCTTGT
	Reverse	CATTAGCGCATCACAGTCGC
cyclin D1	Forward	CTGATTGGACAGGCATGGGT
	Reverse	GTGCCTGGAAGTCAACGGTA
cleaved caspase-9	Forward	AGGCCCCATATGATCGAGGA
	Reverse	TCGACAACTTTGCTGCTTGC
BCL2	Forward	ATAACGGAGGCTGGGTAGGT
	Reverse	TTTATTTCGCCGGCTCCACA

Statistical analysis

Each experiment was triplicated. Data were expressed as mean ± SD and analyzed by GraphPad Prism 7.0 software. Differences were compared by Student's *t*-test or ANOVA. Survival curves were constructed using the Kaplan-Meier method and compared using the log-rank test. Linear correlation was assessed by Pearson correlation analysis. Statistical significance was indicated as $P<0.05$.

Results

Circ_0000284 was overexpressed in ICC tumor tissues and cells

Pathological analysis showed that cancer cells in ICC tumor tissues were disordered and varied in size and

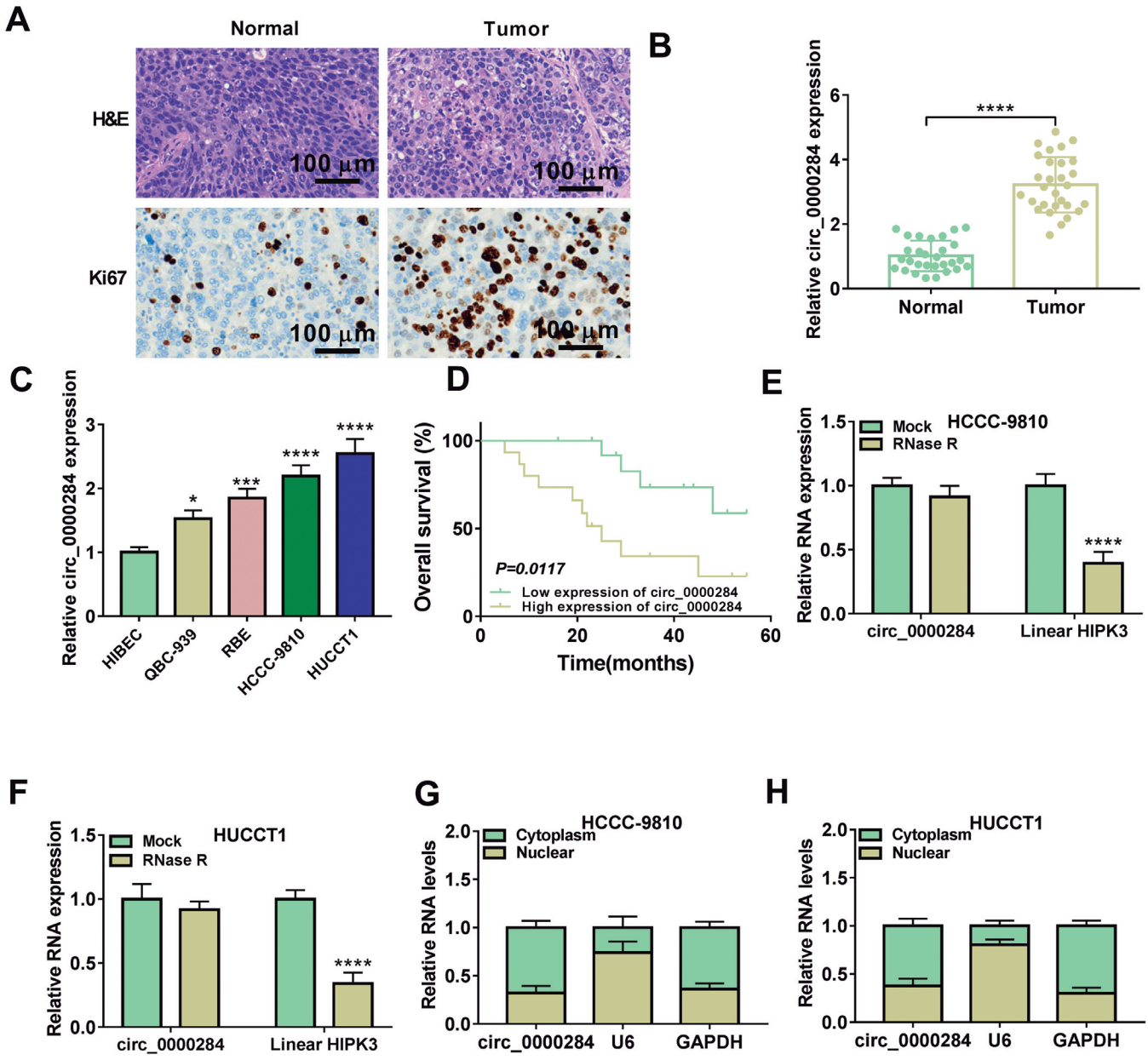

Fig. 1. The expression of circ_0000284 in ICC tumor tissues and cells. **A.** The images of H&E staining and IHC staining for the ICC tumor tissues and adjacent normal tissues. **B.** circ_0000284 expression in ICC tumor tissues and adjacent normal tissues was detected by qRT-PCR. **C.** circ_0000284 expression in ICC cells and HIBEC cells was measured using qRT-PCR. **D.** Kaplan-Meier analysis was used to analyze the correlation between circ_0000284 expression and patients' overall survival rate. RNase R assay **(E, F)** and subcellular localization assay **(G, H)** were performed to measure the circular characteristic of circ_0000284. *P<0.05, ***P<0.001, ****P<0.0001.

shape, and proliferation marker Ki67 positive cells were significantly higher than that in adjacent normal tissues (Fig. 1A). Through analysis, we confirmed that circ_0000284 was highly expressed in ICC tumor tissues compared to adjacent normal tissues (Fig. 1B), and was upregulated in four ICC cells compared with that in HIBEC cells (Fig. 1C). According to the median of circ_0000284 expression, we divided ICC patients into the high circ_0000284 expression group and the low circ_0000284 expression group. We found that patients with high expression of circ_0000284 had a lower overall survival rate than those with low expression of circ_0000284 (Fig. 1D). Through analyzing, we confirmed that circ_0000284 expression was associated with LNM in patients with ICC (Table 1). These results led us to determine that circ_0000284 might be a key regulator of ICC progression. Additionally, we assessed the circular characteristic of circ_0000284 using RNase R assay and subcellular localization assay. The results suggested that circ_0000284 could resist the digestion of

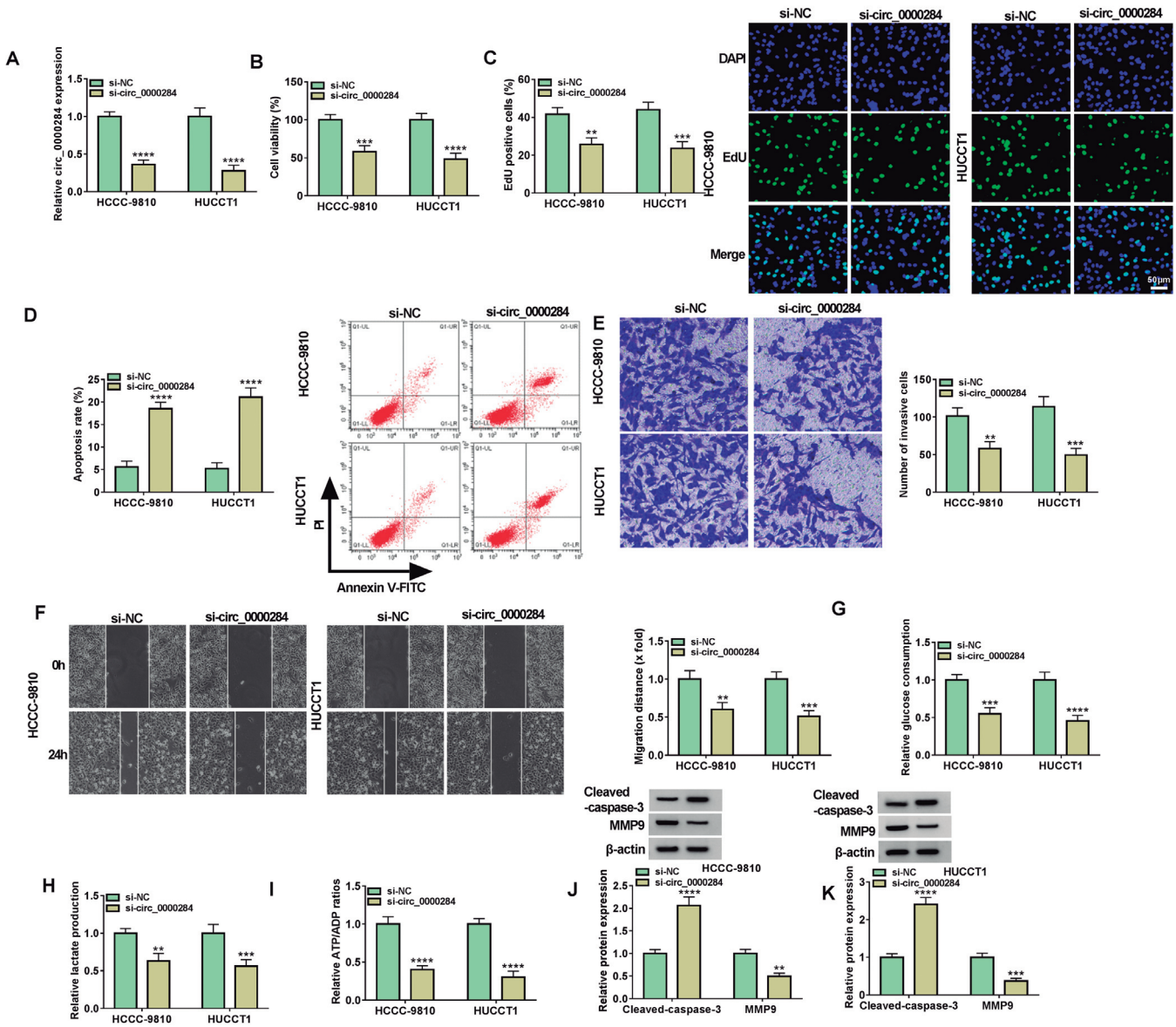

Fig. 2. The regulation of si-circ_0000284 on ICC cell progression. HCCC-9810 and HUCCT1 cells were transfected with si-circ_0000284 or si-NC. **A.** circ_0000284 expression was examined by qRT-PCR. CCK8 assay **(B)**, EdU assay **(C)**, flow cytometry **(D)**, transwell assay **(E)** and wound healing assay **(F)** were used to measure cell proliferation, apoptosis, invasion and migration. **G-I.** Glucose consumption, lactate production and ATP/ADP ratios were tested to assess cell glycolysis. **J, K.** WB analysis was used to test protein expression. **P<0.01, ***P<0.001, ****P<0.0001.

RNase R (Fig. 1E,F), and it was mainly distributed in the cytoplasm of ICC cells (Fig. 1G,H).

Interference of circ_0000284 inhibited ICC cell growth, metastasis and glycolysis

After transfection with si-circ_0000284 into HCCC-9810 and HUCCT1 cells, we confirmed that circ_0000284 expression was indeed decreased (Fig. 2A). Our data revealed that circ_0000284 knockdown restrained cell viability and EdU positive cell rate, while it enhanced cell apoptosis rate (Fig. 2B-D). Also, we observed that downregulated circ_0000284 reduced the number of invasive cells, migration distance, glucose consumption, lactate production and ATP/ADP ratios in ICC cells (Fig. 2E-I). WB analysis results showed that apoptosis marker cleaved-caspase-3 protein expression was increased and metastasis marker MMP9 protein expression was decreased in ICC cells transfected with si-circ_0000284 (Fig. 2J,K). Besides, we found that circ_0000284 knockdown enhanced P21 and cleaved-caspase 9 expression, while it decreased cyclin D1 and BCL2 expression in ICC cells (Fig. 3A,B). The above data indicated that circ_0000284 might promote ICC cell growth, metastasis and glycolysis to accelerate ICC progression.

Circ_0000284 acted as a sponge for miR-152-3p

In the previous study, we screened 6 top-ranked miRNAs as candidate miRNAs according to starbase software. After circ_0000284 knockdown, we detected the expression of each miRNA and found that miR-152-3p expression was most significantly up-regulated (Fig. 4A,B). Therefore, miR-152-3p was selected as the target of circ_0000284 for research. The binding sites between circ_0000284 and miR-152-3p are shown in Fig. 5A. In dual-luciferase reporter assay, the luciferase activity was decreased when miR-152-3p mimic and the WT-circ_0000284 vector were co-transfected (Fig. 5B,C), confirming the interaction between miR-152-3p and circ_0000284. MiR-152-3p was under-expressed in ICC tumor tissues, and its expression was negatively correlated with circ_0000284 expression (Fig. 5D,E). The low miR-152-3p expression also was observed in ICC cells compared to HIBEC cells (Fig. 5F). After overexpressed circ_0000284 expression using circ_0000284 overexpression vector (Fig. 5G), we

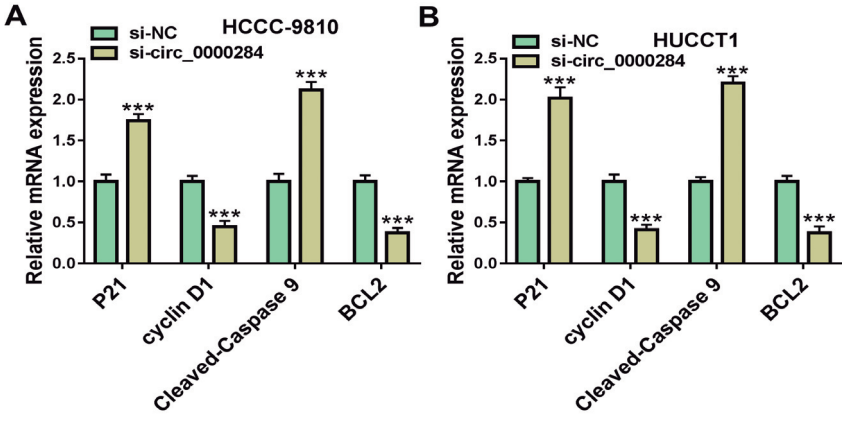

Fig. 3. Effect of circ_0000284 knockdown on mRNA expression. **A, B.** HCCC-9810 and HUCCT1 cells were transfected with si-NC or si-circ_0000284. The mRNA expression of P21, cyclin D1, cleaved-caspase 9 and BCL2 was analyzed by qRT-PCR. ***P<0.001.

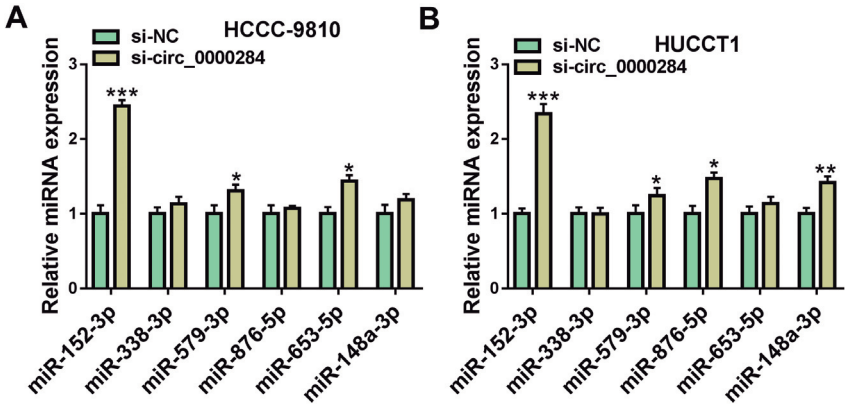

Fig. 4. Screening of targeted miRNA of circ_0000284. **A, B.** HCCC-9810 and HUCCT1 cells were transfected with si-NC or si-circ_0000284. The expression of candidate miRNAs was analyzed by qRT-PCR. *P<0.05, **P<0.01, ***P<0.001.

measured miR-152-3p expression in ICC cells transfected with si-circ_0000284 or circ_0000284 overexpression vector. As shown in Fig. 5H, miR-152-3p expression could be increased by circ_0000284 knockdown and decreased by circ_0000284 overexpression.

The regulation of si-circ_0000284 on ICC cell progression was reversed by anti-miR-152-3p

To further confirm whether the circ_0000284/miR-152-3p axis regulated ICC progression, si-circ_0000284 and anti-miR-152-3p were co-transfected into HCCC-9810 and HUCCT1 cells. Firstly, we verified that the increasing of si-circ_0000284 on miR-152-3p expression was eliminated by anti-miR-152-3p (Fig. 6A). After co-transfection, the inhibitory effects of circ_0000284 knockdown on cell viability and EdU positive cell rate, as well as the promotion effect on cell apoptosis rate were reversed by miR-152-3p inhibitor (Fig. 6B-D). Furthermore, the inhibition effect of si-circ_0000284 on the number of invasive cells, migration distance, glucose consumption, lactate production and ATP/ADP ratios also were overturned by miR-152-3p inhibitor (Fig. 6E-

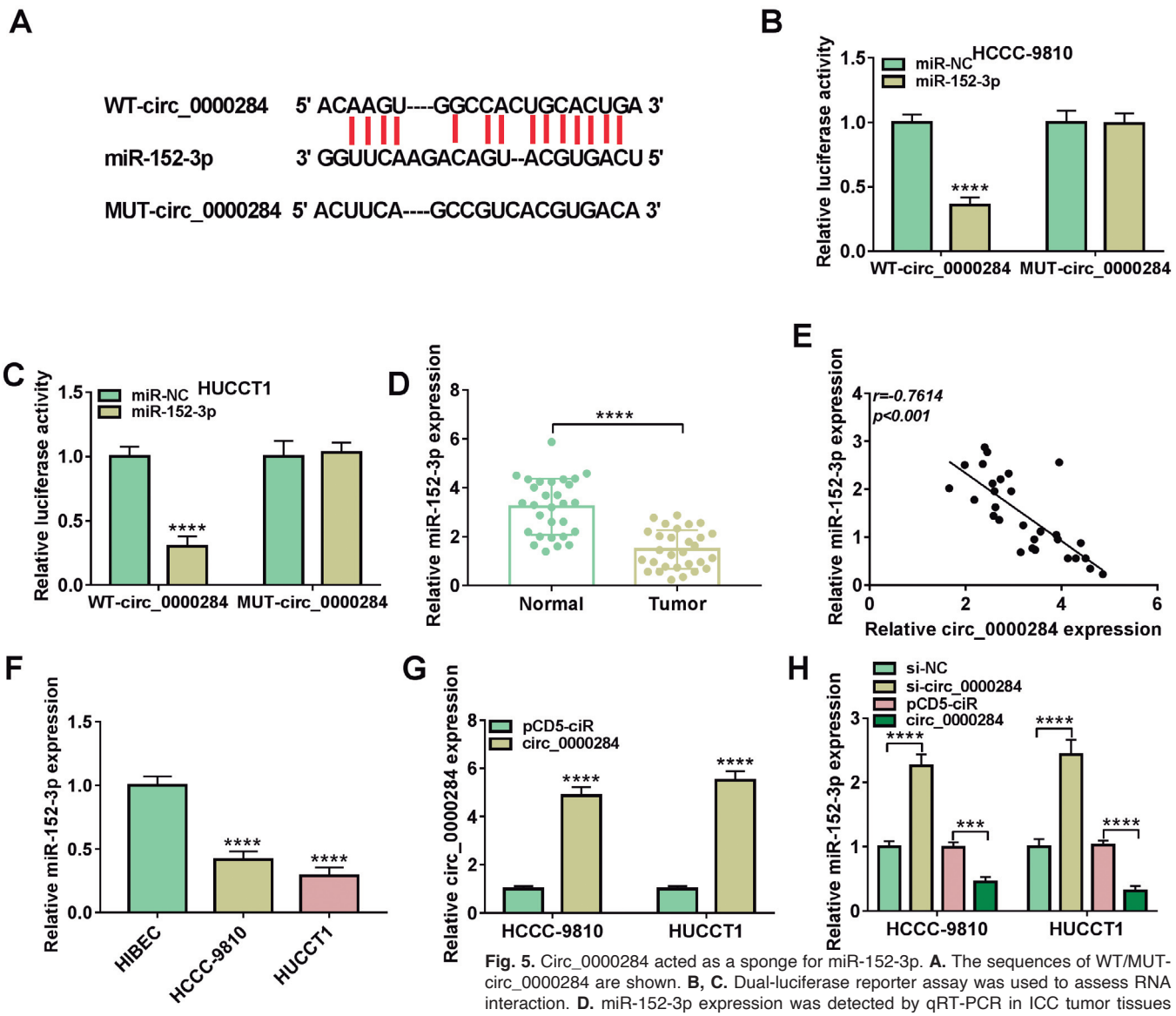

Fig. 5. Circ_0000284 acted as a sponge for miR-152-3p. **A.** The sequences of WT/MUT-circ_0000284 are shown. **B, C.** Dual-luciferase reporter assay was used to assess RNA interaction. **D.** miR-152-3p expression was detected by qRT-PCR in ICC tumor tissues and adjacent normal tissues. **E.** Pearson correlation analysis was used to assess the correlation between miR-152-3p and circ_0000284 expression. **F.** miR-152-3p expression was measured using qRT-PCR in ICC cells and HIBEC cells. **G.** The transfection efficiency of pCD5 circ_0000284 overexpression vector was confirmed by qRT-PCR. **H.** miR-152-3p expression was detected by qRT-PCR in HCCC-9810 and HUCCT1 cells transfected with si-circ_0000284 or circ_0000284 overexpression vector. ***P<0.001, ****P<0.0001.

I). In the co-transfection group, we found that cleaved-caspase-3 protein expression was reduced and MMP9 protein expression was enhanced compared to the si-circ_0000284+anti-miR-NC group (Fig. 6J,K). HK2, pyruvate kinase muscle isozyme M2 (PKM2), and lactate dehydrogenase A (LDHA) are critical glycolysis regulators. Here, we detected HK2, PKM2, GAPDH and LDHA expression. The results showed that

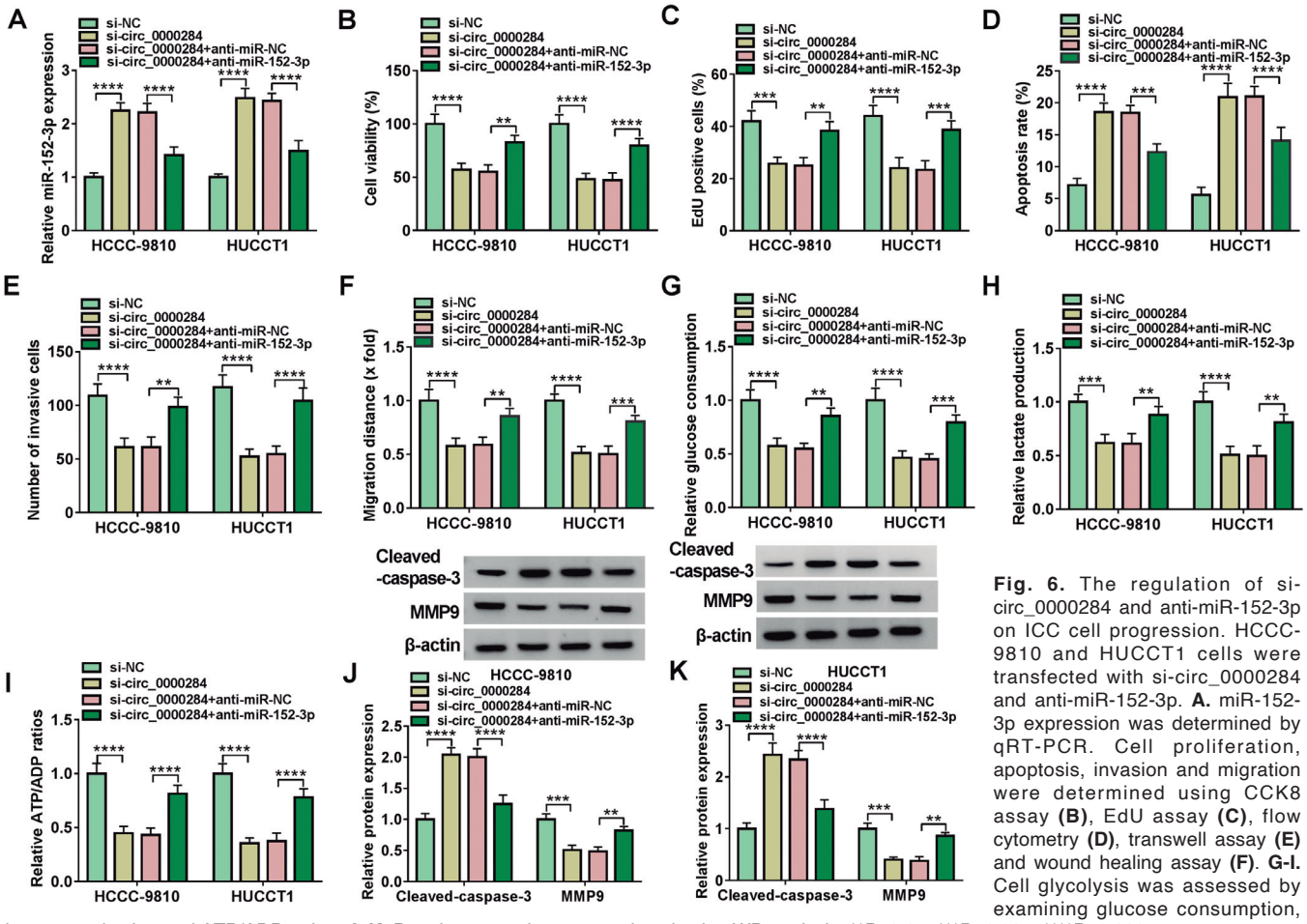

Fig. 6. The regulation of si-circ_0000284 and anti-miR-152-3p on ICC cell progression. HCCC-9810 and HUCCT1 cells were transfected with si-circ_0000284 and anti-miR-152-3p. **A.** miR-152-3p expression was determined by qRT-PCR. Cell proliferation, apoptosis, invasion and migration were determined using CCK8 assay **(B)**, EdU assay **(C)**, flow cytometry **(D)**, transwell assay **(E)** and wound healing assay **(F)**. **G-I.** Cell glycolysis was assessed by examining glucose consumption, lactate production and ATP/ADP ratios. **J, K.** Protein expression was analyzed using WB analysis. **P<0.01, ***P<0.001, ****P<0.0001.

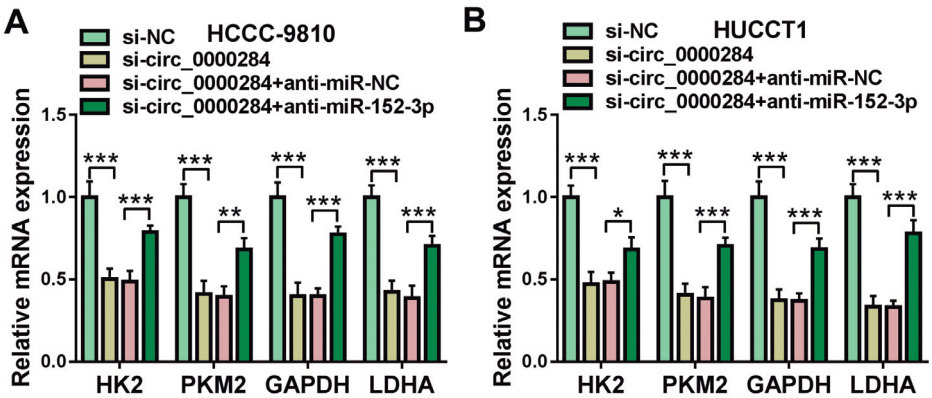

Fig. 7. Effect of circ_0000284 knockdown and miR-152-3p inhibitor on glycolysis-related marker expression. **A, B.** HCCC-9810 and HUCCT1 cells were transfected with si-circ_0000284 and anti-miR-152-3p. The mRNA expression of HK2, PKM2, GAPDH and LDHA was analyzed by qRT-PCR. *P<0.05, **P<0.01, ***P<0.001.

circ_0000284 knockdown also repressed HK2, PKM2, GAPDH and LDHA expression, and these effects also were eliminated by miR-152-3p inhibitor (Fig. 7A,B). These data illuminated that circ_0000284 sponged miR-152-3p to facilitate ICC progression.

MiR-152-3p targeted PDK1

Through starbase software, we screened 6 top-ranked mRNAs as candidate mRNAs. In ICC cells transfected with anti-miR-152-3p, we found that PDK1 expression was most significantly upregulated among them (Fig. 8A,B). Therefore, PDK1 was selected as the target of miR-152-3p for research. The binding sites between PDK1 and miR-152-3p are listed in Fig. 9A. Through verification, we confirmed the interaction between miR-152-3p and PDK1, showing that miR-152-3p mimic only reduced the luciferase activity driven by

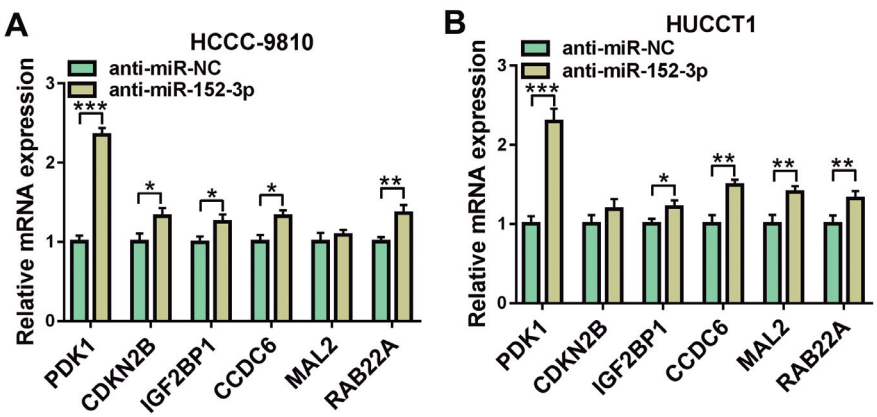

Fig. 8. Screening of targeted mRNA of miR-152-3p. **A, B.** HCCC-9810 and HUCCT1 cells were transfected with anti-miR-NC or anti-miR-152-3p. The expression of candidate mRNAs was analyzed by qRT-PCR. *P<0.05, **P<0.01, ***P<0.001.

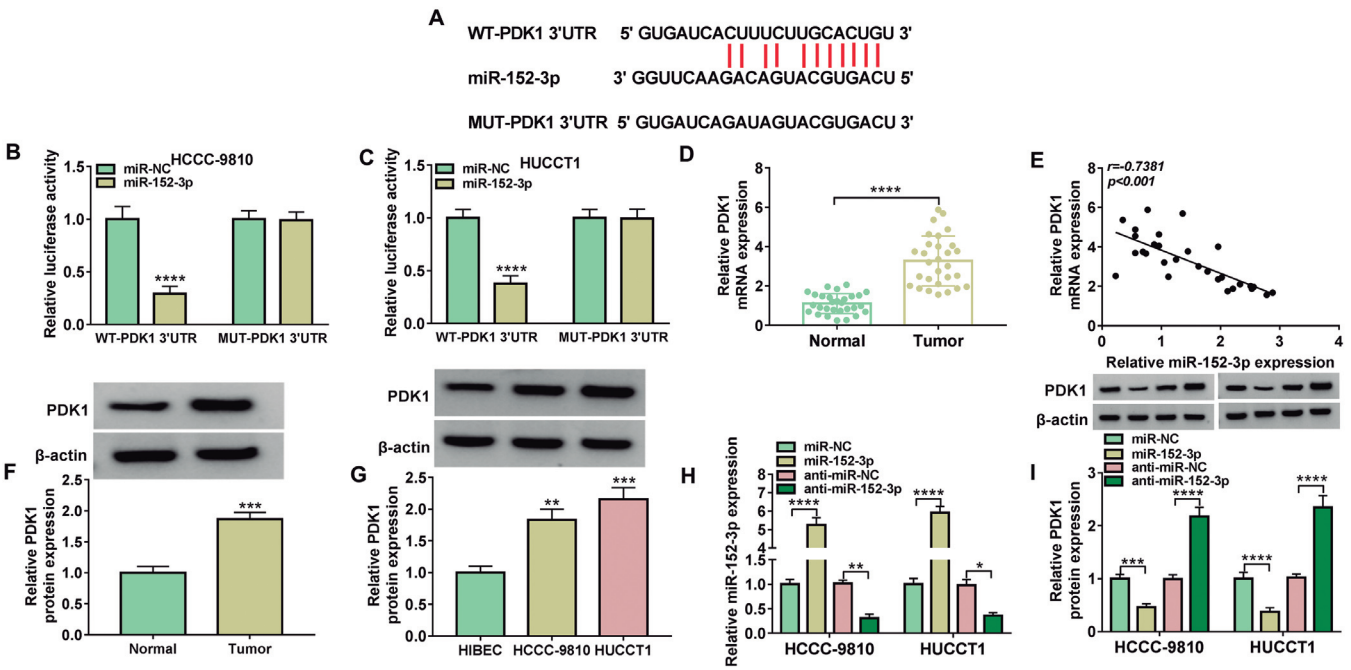

Fig. 9. MiR-152-3p targeted PDK1. **A.** The sequences of WT/MUT-PDK1 3'UTR are shown. **B, C.** RNA interaction was evaluated using dual-luciferase reporter assay. **D.** PDK1 mRNA expression was examined by qRT-PCR in ICC tumor tissues and adjacent normal tissues. **E.** Pearson correlation analysis was performed to evaluate the correlation between PDK1 and miR-152-3p expression. **F.** PDK1 protein expression in ICC tumor tissues and adjacent normal tissues was determined by WB analysis. **G.** PDK1 protein expression was analyzed using WB analysis in ICC cells and HIBEC cells. **H.** The transfection efficiencies of miR-152-3p mimic and inhibitor were confirmed by qRT-PCR. **I.** PDK1 protein expression was detected by WB analysis in HCCC-9810 and HUCCT1 cells transfected with miR-152-3p mimic or inhibitor. *P<0.05, **P<0.01, ***P<0.001, ****P<0.0001.

the WT-PDK1 3'UTR vector (Fig. 9B,C). PDK1 mRNA expression was upregulated in ICC tumor tissues and was negatively correlated with miR-152-3p expression (Fig. 9D,E). The results of WB analysis revealed that PDK1 protein expression was higher in ICC tumor tissues and cells than that in corresponding controls (Fig.

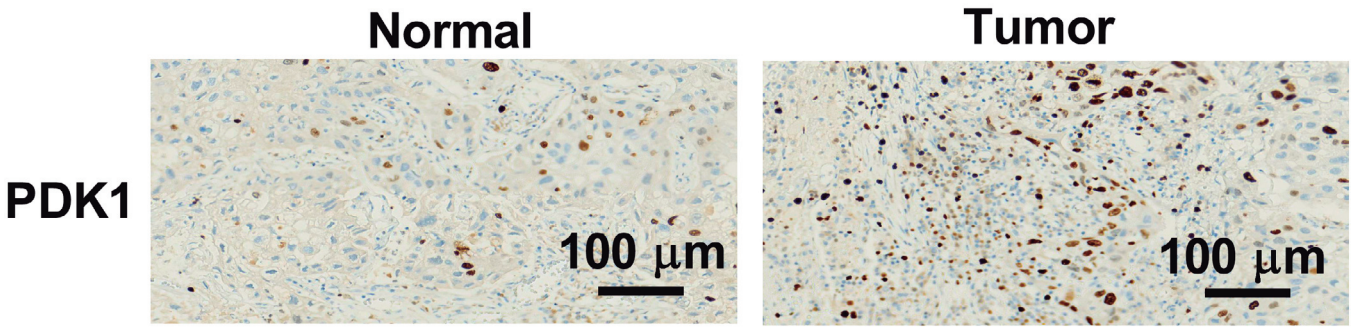

Fig. 10. PDK1 positive cells detected by IHC staining. IHC staining was used to analyze PDK1 positive cells in ICC tumor tissues and adjacent normal tissues.

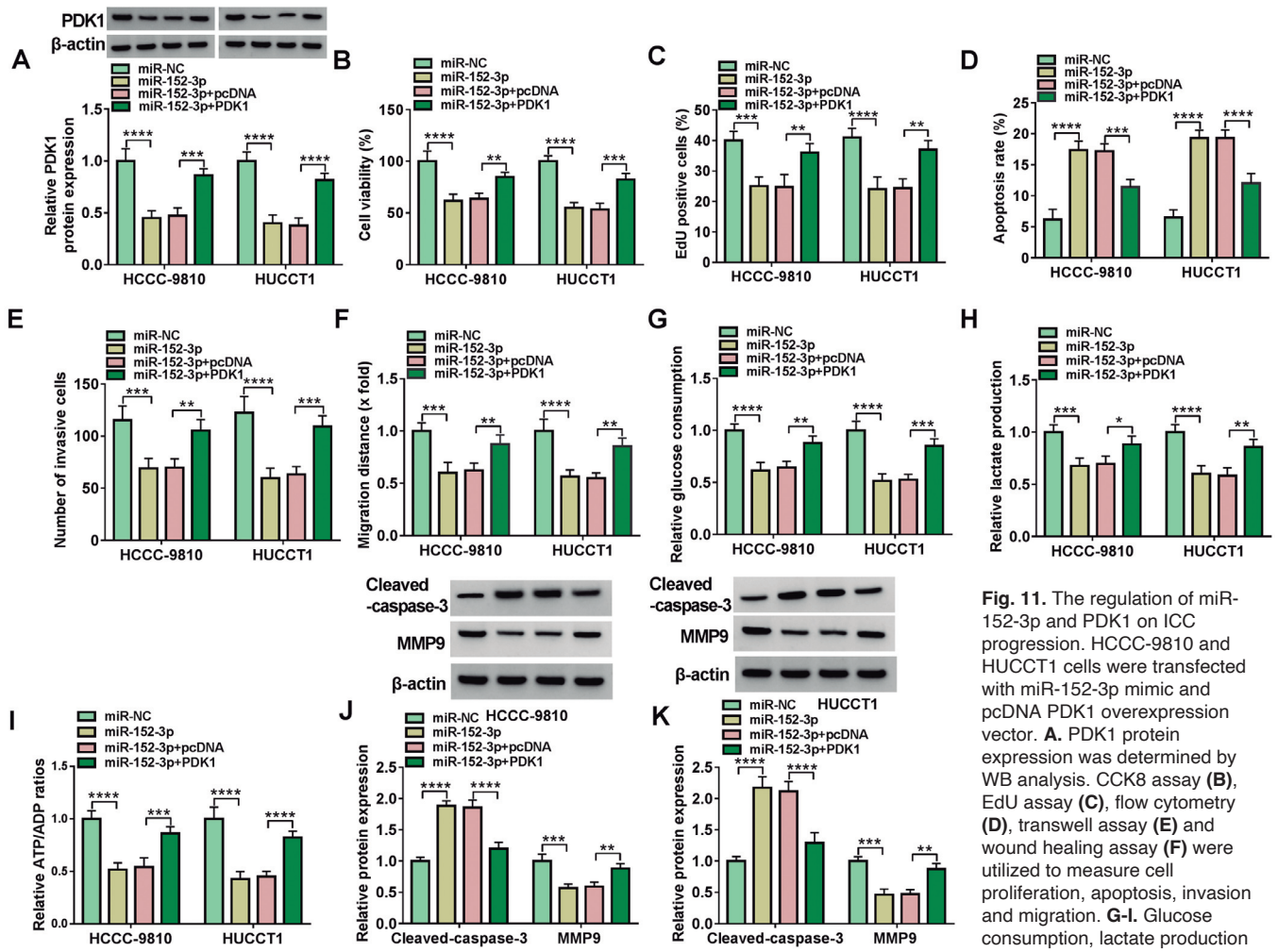

Fig. 11. The regulation of miR-152-3p and PDK1 on ICC progression. HCCC-9810 and HUCCT1 cells were transfected with miR-152-3p mimic and pcDNA PDK1 overexpression vector. **A.** PDK1 protein expression was determined by WB analysis. CCK8 assay **(B)**, EdU assay **(C)**, flow cytometry **(D)**, transwell assay **(E)** and wound healing assay **(F)** were utilized to measure cell proliferation, apoptosis, invasion and migration. **G-I.** Glucose consumption, lactate production and ATP/ADP ratios were analyzed to evaluate cell glycolysis. **J, K.** Protein expression was examined by WB analysis. *P<0.05, **P<0.01, ***P<0.001, ****P<0.0001.

9F,G). Then, miR-152-3p mimic was confirmed to promote miR-152-3p expression and its inhibitor was verified to inhibit miR-152-3p expression (Fig. 9H). By detecting PDK1 protein expression, we observed that PDK1 expression was suppressed by miR-152-3p overexpression, while it was promoted by miR-152-3p inhibitor (Fig. 9I). Besides, IHC staining confirmed that PDK1 positive cells were enhanced in ICC tumor tissues compared to adjacent normal tissues (Fig. 10).

MiR-152-3p repressed ICC progression by targeting PDK1

Subsequently, we performed rescue experiments to confirm that miR-152-3p targeted PDK1 to regulate ICC progression. After transfection with miR-152-3p mimic and pcDNA PDK1 expression vector into HCCC-9810 and HUCCT1 cells, the decrease of miR-152-3p mimic on PDK1 protein expression was abolished by the addition of pcDNA PDK1 expression vector (Fig. 11A). The present data showed that miR-152-3p mimic inhibited cell viability, repressed EdU positive cell rate and promoted cell apoptosis rate, while these effects were rescued by PDK1 overexpression (Fig. 11B-D). Upregulation of PDK1 reversed the inhibiting effects of miR-152-3p on the number of invasive cells, migration distance, glucose consumption, lactate production and ATP/ADP ratios (Fig. 11E-I). MiR-152-3p mimic also enhanced cleaved-caspase-3 protein expression and repressed MMP9 protein expression, and PDK1 overexpression revoked this effect (Fig. 11J,K). Additionally, miR-152-3p decreased HK2, PKM2, GAPDH and LDHA expression, and PDK1 overexpression also reversed this effect (Fig. 12A,B).

Circ_0000284 regulated PDK1 via sponging miR-152-3p

To reveal the regulation of circ_0000284 on PDK1, we examined PDK1 mRNA and protein expression under different treatment conditions. According to our results, circ_0000284 knockdown reduced PDK1 mRNA and protein expression in HCCC-9810 and HUCCT1 cells, and the addition of anti-miR-152-3p reversed these effects (Fig. 13A,B). Therefore, our data determined that circ_0000284 sponged miR-152-3p to regulate PDK1.

Knockdown of circ_0000284 inhibited the growth of ICC tumors in vivo

To determine the role of circ_0000284 *in vivo*, we constructed HUCCT1 cells with stable knockdown of circ_0000284 (Fig. 14A). Then, the transfected cells were injected into mice for 22 days. The tumor volume and weight were reduced in the sh-circ_0000284 group (Fig. 14B,C), suggesting that circ_0000284 might promote ICC tumor growth. In the tumor tissues of sh-circ_0000284 group, we confirmed that circ_0000284 expression was decreased, miR-152-3p expression was increased, and PDK1 protein expression was suppressed (Fig. 14D,E). Moreover, the results of IHC staining revealed that PDK1, Ki67 and MMP9 positive cells were reduced in the tumor tissues of the sh-circ_0000284 group (Fig. 14F).

Discussion

Compared with hepatocellular carcinoma (HCC), ICC has a more insidious onset, rapid progress, and a higher degree of malignancy (Mejia and Pasko, 2020). Like other malignant tumors, the pathogenesis of ICC is not clear, but primary sclerosing cholangitis and fatty liver are considered to be important risk factors for ICC occurrence (Taghavi et al., 2018; Corrao et al., 2021). Understanding the molecular mechanisms that influence ICC progression may provide potential therapeutic targets for ICC. Here, we selected a circRNA that had been reported to be upregulated in cholangiocarcinoma for study. Our data indicated that circ_0000284 was overexpressed in ICC. Circ_0000284 knockdown repressed ICC cell growth, metastasis and glycolysis, and hindered tumor growth *in vivo*. This evidence confirmed that circ_0000284 contributed to ICC

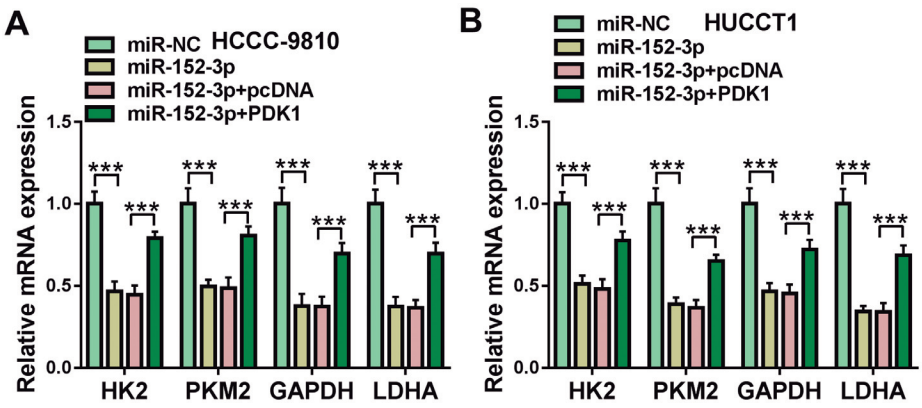

Fig. 12. Effect of miR-152-3p and PDK1 on glycolysis-related marker expression. **A, B.** HCCC-9810 and HUCCT1 cells were transfected with miR-152-3p mimic or PDK1 overexpression vector. The mRNA expression of HK2, PKM2, GAPDH and LDHA was detected by qRT-PCR. ***P<0.001.

malignant progression, which was similar to previous studies (Wang et al., 2019). Not only that, we also determined that circ_0000284 had a carcinogenic effect in ICC, which was consistent with its role in other cancers (Li et al., 2020b; Qi et al., 2021).

Mechanically, we pointed out that circ_0000284 might serve as a miR-152-3p sponge. By referring to the literature, miR-152-3p was significantly underexpressed in a variety of cancers and had a tumor suppressive role in cancer progression, such as in lung cancer (Huang et al., 2021) and endometrial carcinoma (Liang et al., 2021). Research had reported that miR-152-3p was associated with HCC progression, which mediated the inhibition on epithelial mesenchymal transition in HCC (Li et al., 2021a). A previous study confirmed the low miR-152-3p expression in ICC tissues, and illuminated that inhibition of miR-152-3p enhanced ICC cell metastasis (Braconi et al., 2010). Consistent with these data, we verified the anti-cancer role of miR-152-3p in ICC, showing that its overexpression restrained ICC cell growth, metastasis and glycolysis. Also, anti-miR-152-3p overturned the effects of si-circ_0000284 on ICC cell malignant phenotype, which confirmed the circ_0000284/miR-152-3p axis in ICC.

PDK1 is a regulator of pyruvate dehydrogenase, a key rate-limiting enzyme of cellular glycolysis, and has been widely confirmed to be involved in regulating cancer progression (Sheng et al., 2021; Wu et al., 2021). Research had revealed that high PDK1 expression was correlated with the poor prognosis of ovarian cancer patients, and its interference suppressed cancer proliferation and metastasis (Yao et al., 2021). A recent

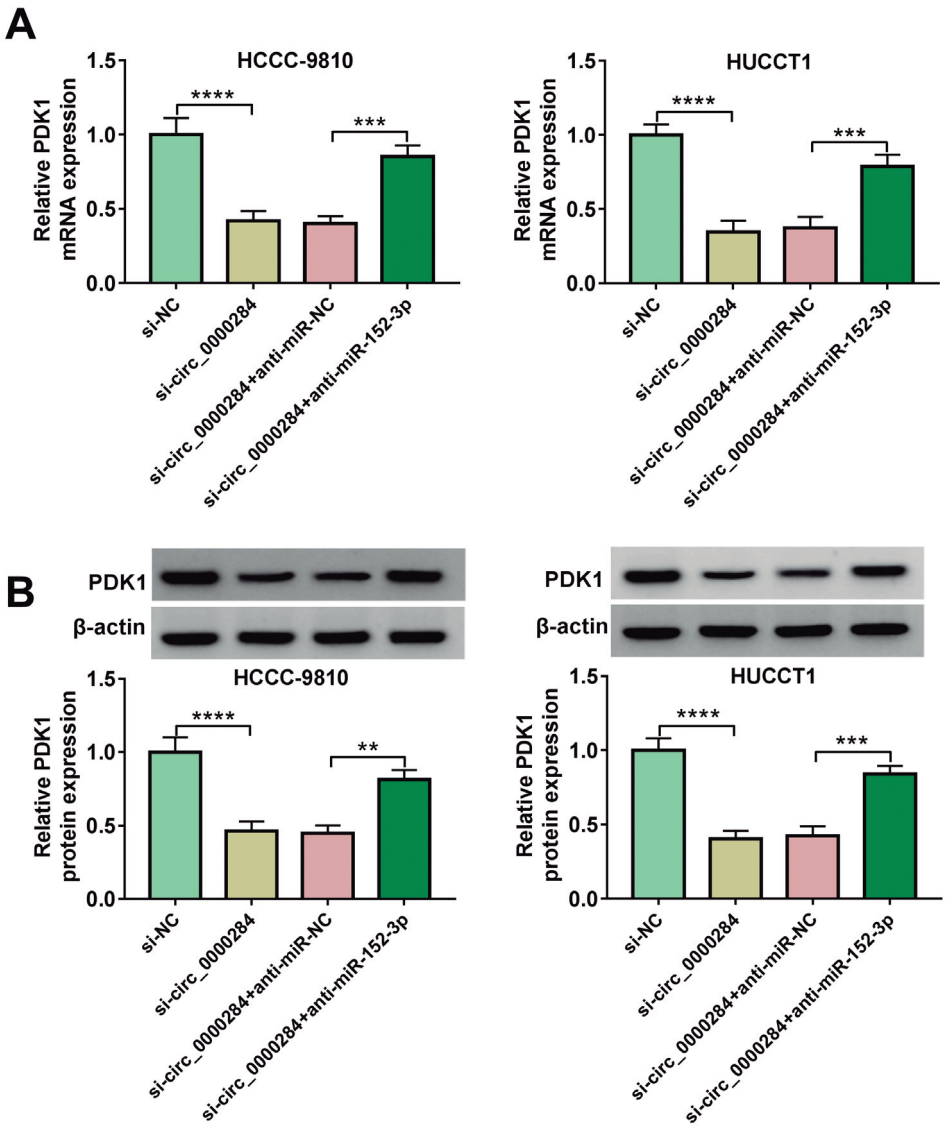

Fig. 13. The regulation of circ_0000284 and miR-152-3p on PDK1 expression. PDK1 mRNA and protein expression was measured by qRT-PCR **(A)** and WB analysis **(B)** in HCCC-9810 and HUCCT1 cells transfected with si-circ_0000284 and anti-miR-152-3p. **P<0.01, ***P<0.001, ****P<0.0001.

study showed that upregulated PDK1 contributed to cholangiocarcinoma cell growth and metastasis (Li et al., 2021b). Also, inhibition of PDK1-mediated signaling pathway had been suggested to hinder cholangiocarcinoma cell growth and tumorigenesis (Xu et al., 2019). Here, we confirmed the overexpressed PDK1 in ICC tissues and cells, and indicated that its upregulation rescued the inhibition of miR-152-3p on ICC cell development. These verified that miR-152-3p restrained ICC progression by targeting PDK1. In addition, we also revealed the regulatory role of circ_0000284 on PDK1 expression, which improved the results of circ_0000284/miR-152-3p/PDK1 axis.

In conclusion, circ_0000284 played an oncogene role in ICC, which facilitated ICC growth, metastasis and glycolysis through sponging miR-152-3p to increase PDK1 expression. These findings suggested that targeting the circ_0000284/miR-152-3p/PDK1 axis

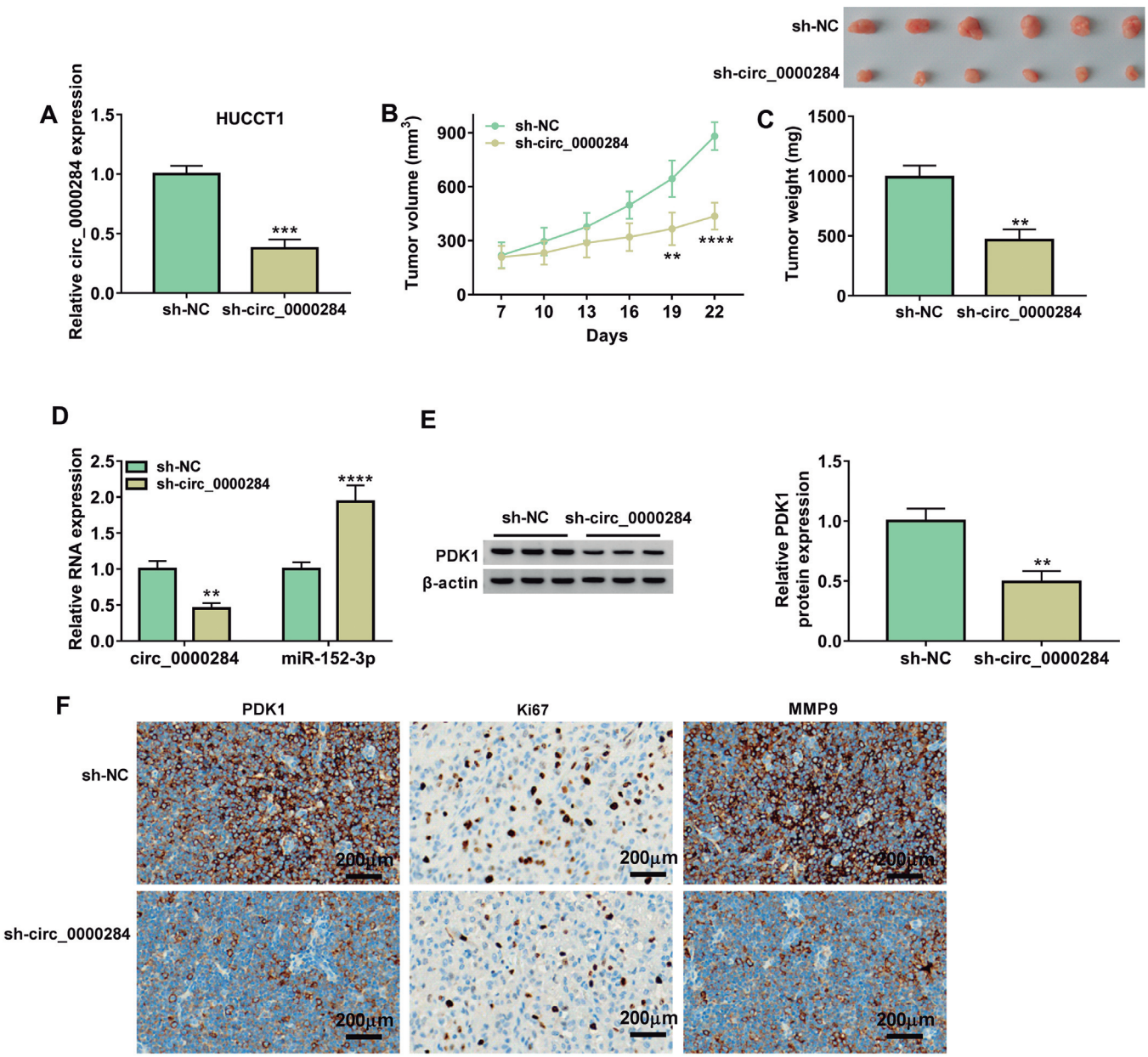

Fig. 14. The regulation of sh-circ_0000284 on ICC tumor growth. **A.** The transfection efficiency of sh-circ_0000284 was confirmed by qRT-PCR. (B-F) HUCCT1 cells transfected with sh-circ_0000284 or sh-NC were injected into nude mice. Tumor volume **(B)** and weight **(C)** were determined. **D.** The expression of circ_0000284 and miR-152-3p in the tumor tissues of mice was detected by qRT-PCR. **E.** PDK1 protein expression in the tumor tissues of mice was measured by WB analysis. **F.** IHC staining was used to measure PDK1, Ki67 and MMP9 positive cells in the tumor tissues of mice. **P<0.01, ***P<0.001, ****P<0.0001.

might be a novel therapeutic strategy for ICC.

Acknowledgements. Not applicable.

Ethics approval and consent to participate. The present study was approved by the ethical review committee of Hanchuan People's Hospital. Written informed consent was obtained from all enrolled patients.

Consent for publication. Patients agree to participate in this work.

Availability of data and materials. The analyzed data sets generated during the present study are available from the corresponding author on reasonable request.

Competing interests. The authors declare that they have no competing interests.

Funding. No funding was received.

References

Altesha M.A., Ni T., Khan A., Liu K. and Zheng X. (2019). Circular RNA in cardiovascular disease. J. Cell Physiol. 234, 5588-5600.

Braconi C., Huang N. and Patel T. (2010). MicroRNA-dependent regulation of DNA methyltransferase-1 and tumor suppressor gene expression by interleukin-6 in human malignant cholangiocytes. Hepatology 51, 881-890.

Chen B. and Huang S. (2018). Circular RNA: An emerging non-coding RNA as a regulator and biomarker in cancer. Cancer Lett. 418, 41-50.

Chen L.L. (2020). The expanding regulatory mechanisms and cellular functions of circular RNAs. Nat. Rev. Mol. Cell Biol. 21, 475-490.

Chen Q., Wang H., Li Z., Li F., Liang L., Zou Y., Shen H., Li J., Xia Y., Cheng Z., Yang T., Wang K. and Shen F. (2021). Circular RNA ACTN4 promotes intrahepatic cholangiocarcinoma progression by recruiting YBX1 to initiate FZD7 transcription. J. Hepatol. 76, 135-147.

Corrao S., Natoli G. and Argano C. (2021). Nonalcoholic fatty liver disease is associated with intrahepatic cholangiocarcinoma and not with extrahepatic form: definitive evidence from meta-analysis and trial sequential analysis. Eur. J. Gastroenterol. Hepatol. 33, 62-68.

El-Diwany R., Pawlik T.M. and Ejaz A. (2019). Intrahepatic cholangiocarcinoma. Surg. Oncol. Clin. N. Am. 28, 587-599.

Hogdall D., O'Rourke C.J., Taranta A., Oliveira D.V. and Andersen J.B. (2016). Molecular pathogenesis and current therapy in intrahepatic cholangiocarcinoma. Dig. Dis. 34, 440-451.

Huang J., Lou J., Liu X. and Xie Y. (2021). LncRNA PCGsEM1 contributes to the proliferation, migration and invasion of Non-small cell lung cancer cells via acting as a sponge for miR-152-3p short title: The PCGEM1/miR-152-3p axis in NSCLC. Curr. Pharm. Des. 27, 4663-4670.

Lee A.J. and Chun Y.S. (2018). Intrahepatic cholangiocarcinoma: the AJCC/UICC 8th edition updates. Chin. Clin. Oncol. 7, 52.

Lei B., Tian Z., Fan W. and Ni B. (2019) Circular RNA: a novel biomarker and therapeutic target for human cancers. Int. J. Med. Sci. 16, 292-301.

Li T.R., Jia Y.J., Wang Q., Shao X.Q. and Lv R.J. (2017). Circular RNA: a new star in neurological diseases. Int. J. Neurosci. 127, 726-734.

Li J., Sun D., Pu W., Wang J. and Peng Y. (2020a). Circular RNAs in cancer: Biogenesis, function, and clinical significance. Trends Cancer. 6, 319-336.

Li L., Zhang Q. and Lian K. (2020b). Circular RNA circ_0000284 plays an oncogenic role in the progression of non-small cell lung cancer through the miR-377-3p-mediated PD-L1 promotion. Cancer Cell Int. 20, 247.

Li H., Wu Y., Wang R., Guo J., Yu Q., Zhang L., Zhao H. and yang H. (2021a). LncSNHG3 promotes hepatocellular carcinoma epithelial mesenchymal transition progression through the miR-152-3p/JAK1 pathway. Genes Genomics 44, 133-144.

Li J., Guan C., Hu Z., Liu L., Su Z., Kang P., Jiang Z. and Cui Y. (2021b). Yin Yang 1-induced LINC00667 up-regulates pyruvate dehydrogenase kinase 1 to promote proliferation, migration and invasion of cholangiocarcinoma cells by sponging miR-200c-3p. Hum. Cell. 34, 187-200.

Liang M., Wang H., Liu C., Lei T. and Min J. (2021). OIP5-AS1 contributes to the development in endometrial carcinoma cells by targeting miR-152-3p to up-regulate SLC7A5. Cancer Cell Int. 21, 440.

Liu Q., Zhang W., Wu Z., Liu H., Hu H., Shi H., Li S. and Zhang X. (2020). Construction of a circular RNA-microRNA-messengerRNA regulatory network in stomach adenocarcinoma. J. Cell Biochem. 121, 1317-1331.

Mavros M.N., Economopoulos K.P., Alexiou V.G. and Pawlik T.M. (2014). Treatment and prognosis for patients with intrahepatic cholangiocarcinoma: systematic review and meta-analysis. JAMA Surg. 149, 565-574.

Mejia J.C. and Pasko J. (2020). Primary liver cancers: Intrahepatic cholangiocarcinoma and hepatocellular carcinoma. Surg. Clin. North Am. 100, 535-549.

Moeini A., Sia D., Bardeesy N., Mazzaferro V. and Llovet J.M. (2016). Molecular pathogenesis and targeted therapies for intrahepatic cholangiocarcinoma. Clin. Cancer Res. 22, 291-300.

Qi L., Sun B., Yang B. and Lu S. (2021). circHIPK3 (hsa_circ_0000284) promotes proliferation, migration and invasion of breast cancer cells via miR-326. Onco. Targets Ther. 14, 3671-3685.

Sheng W., Xu W., Ding J., Li L., You X., Wu Y. and He Q. (2021). Curcumol inhibits the malignant progression of prostate cancer and regulates the PDK1/AKT/mTOR pathway by targeting miR9. Oncol. Rep. 46, 246.

Taghavi S.A., Eshraghian A., Niknam R., Sivandzadeh G.R. and Lankarani K.B. (2018). Diagnosis of cholangiocarcinoma in primary sclerosing cholangitis. Expert Rev. Gastroenterol. Hepatol. 12, 575-584.

Wang S., Hu Y., Lv X., Li B., Gu D., Li Y., Sun Y. and Su Y. (2019). Circ-0000284 arouses malignant phenotype of cholangiocarcinoma cells and regulates the biological functions of peripheral cells through cellular communication. Clin. Sci. (Lond). 133, 1935-1953.

Wu J., Liu S., Xiang Y., Qu X., Xie Y. and Zhang X. (2019). Bioinformatic analysis of circular RNA-Associated ceRNA network associated with hepatocellular Carcinoma. Biomed. Res. Int. 2019, 8308694.

Wu K., Wang Z., Huang Y., Yao L., Kang N., Ge W., Zhang R. and He W. (2021). LncRNA PTPRG-AS1 facilitates glycolysis and stemness properties of esophageal squamous cell carcinoma cells through miR-599/PDK1 axis. J. Gastroenterol. Hepatol. 37, 507-517.

Xu Y.P., Dong Z.N., Wang S.W., Zheng Y.M., Zhang C., Zhou Y.Q., Zhao Y.J., Zhao Y., Wang F., Peng R., Tang M.C., Bai D.S., Huang X.Y. and Guo C.Y. (2021). circHMGCS1-016 reshapes immune environment by sponging miR-1236-3p to regulate CD73 and GAL-8 expression in intrahepatic cholangiocarcinoma. J. Exp. Clin. Cancer Res. 40, 290.

Xu L., Li Y., Zhou L., Dorfman R.G., Liu L., Cai R., Jiang C., Tang D., Wang Y., Zou X., Wang L. and Zhang M. (2019). SIRT3 elicited an anti-Warburg effect through HIF1alpha/PDK1/PDHA1 to inhibit cholangiocarcinoma tumorigenesis. Cancer Med. 8, 2380-2391.

Yao S., Shang W., Huang L., Xu R., Wu M. and Wang F. (2021). The oncogenic and prognostic role of PDK1 in the progression and metastasis of ovarian cancer. J. Cancer. 12, 630-643.

Zhang H., Yang T., Wu M. and Shen F. (2016). Intrahepatic cholangiocarcinoma: Epidemiology, risk factors, diagnosis and surgical management. Cancer Lett. 379, 198-205.

Accepted November 4, 2022